Review of Double Beta Experiments

X Sarazin

Review of Double Beta Experiments

2015 J. Phys.: Conf. Ser. 593 012006

(http://iopscience.iop.org/1742-6596/593/1/012006)

Journal of Physics: Conference Series **593** (2015) 012006 doi:10.1088/1742-6596/593/1/012006

Review of Double Beta Experiments

X Sarazin
LAL, IN2P3/CNRS and Univ. Paris Sud
E-mail: sarazin@lal.in2p3.fr

Abstract. This paper gives a review of the double beta experimental techniques and projects, in the search for the Majorana neutrino. The purpose of this review is to detail, for each technique, the different origins of background, how they can be identified, and how they can be reduced. Advantages and limitations of the different techniques are discussed.

1. Introduction

The neutrino is one of the most puzzling elementary particle with very unique properties. It has no electrical charge[1], it is thus only sensitive to weak interaction and its mass is very light. The absence of electrical charge is a major characteristic. Ettore Majorana showed that a neutral elementary particle which does not contain any discrete quantum number (as the neutrino), can be described by a so-called Majorana field, in which the distinction between matter and antimatter vanishes [2]. In other words, a neutrino might be identical to its own anti-particle.

If the neutrino is a Majorana neutrino, an important consequence is that Lepton Number Violation (LNV) must occur [3][4]. LNV is a required condition for Grand Unified Theories (GUT), in which quarks and leptons are components of the same multiplet, and hence both lepton and baryon numbers are not expected to be conserved quantities. Leptogenesis is an example of model, which uses the LNV from the decay of heavy Majorana neutrinos to produce the observed asymetry of matter and antimatter in the Universe. Another motivation for the Majorana neutrino is the see-saw mechanism [5][3], which splits the Majorana mass term of neutrinos in light and heavy Majorana neutrinos and thus could explain the very small mass of the observed neutrinos, with the condition that the mass of the heavy one is at the GUT energy scale of about 10^{15} GeV.

The most sensitive method to answer the nature of the neutrino is the search of the neutrinoless double beta decay ($\beta\beta0\nu$).

2. The neutrinoless double beta decay

The standard double beta decay with emission of two electrons and two neutrinos ($\beta\beta2\nu$) is a second order process of β-decay, which is produced by isotopes whose β-decay is forbidden or strongly suppressed:

$$(A, Z) \rightarrow (A, Z-2) + 2e^- + 2\nu_e$$

[1] The limit on the $\bar{\nu}_e$ magnetic moment gives $q/e < 3.7\ 10^{-12}$ and astrophysical considerations give $q/e < 2\ 10^{-14}$ [1]

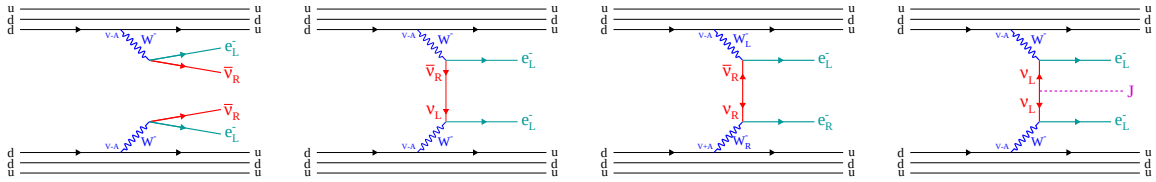

Figure 1. Feynman diagram of the double beta processes. From left to right: standard $\beta\beta$-decay with emission of two neutrinos; $\beta\beta0\nu$-decay with exchange of a virtual Majorana neutrino; $\beta\beta0\nu$-decay with right handed weak coupling; $\beta\beta0\nu$-decay with a Majoron emission.

This standard process is very rare and has been already observed for 7 isotopes with a half-life varying from about 7 10^{18} years for ^{100}Mo and ^{150}Nd, to about 10^{21} years for ^{76}Ge and ^{136}Xe, and about 2 10^{24} years for ^{128}Te. Table 1 lists the double beta isotopes used in the search of the $\beta\beta0\nu$-decay and their measured $\beta\beta2\nu$ half-life.

If we now consider that the neutrino is a Majorana particle, then it becomes possible that the neutrino emitted at the first vertex of the W boson decay is absorbed by the second W vertex and thus only two electrons are emitted by the nucleus, as illustrated in Figure 1. It corresponds to the neutrinoless double beta decay ($\beta\beta0\nu$) where two neutrons decay into two protons emitting only two electrons:

$$(A, Z) \rightarrow (A, Z-2) + 2e^-$$

This process violates the lepton number by two units ($\Delta L = 2$), and is thus forbidden by the Standard Model.

Experimentally, the two decay modes, $\beta\beta2\nu$ and $\beta\beta0\nu$ are distinguished by the fact that the energy sum of the two electrons in $\beta\beta0\nu$-decay is constant and equal to the transition energy $Q_{\beta\beta}$ while it varies continuously in $\beta\beta2\nu$-decay up to the same energy as its limit (with a maximum around 1/3 $Q_{\beta\beta}$), as illustrated in Figure 2.

Other mechanisms which violate the lepton number conservation can also induce $\beta\beta0\nu$ decay and contribute to its amplitude: a right-handed component in the weak interaction, the exchange of a supersymmetric particle with short-range or long-range R-parity violating SUSY contributions, or the emission of a Majoron, a goldstone (massless) boson related to the $L-B$ symmetry breaking (see Figure 1). In the latest case, the $\beta\beta$ energy sum spectrum of the two electrons is expected to be distorted. The deformation depends on the spectral index (or number of emitted Majoron). A complete review of possible mechanisms is given in [6].

Even if many mechanisms are possible to produce $\beta\beta0\nu$-decay, any observation of $\beta\beta0\nu$-decay would prove that the neutrino is a Majorana particle. This feature is known as the Schechter-Valle theorem [7][4].

If we assume that the dominant lepton number violation mechanism at low energies is the light Majorana neutrino exchange, the half-life of $\beta\beta0\nu$-decay can be written as:

$$\left(T^{0\nu}_{1/2}\right)^{-1} = G_{0\nu}(Q_{\beta\beta}, Z)\,|M_{0\nu}|^2\,\frac{\langle m_{ee}\rangle^2}{m_e^2}$$

where $G_{0\nu}(Q_{\beta\beta}, Z)$ is the phase space factor, which contains the kinematic information about the final state particles, and is exactly calculable to the precision of the input parameters, $|M_{0\nu}|$ is the nuclear matrix element, m_e is the mass of the electron, and $\langle m_{ee}\rangle$ is the effective Majorana mass of the electron neutrino, which is defined as $\langle m_{ee}\rangle = \left|\sum_i U_{ei}^2 m_i\right|$ where m_i are the neutrino mass eigenstates and U_{ei} are the elements of the neutrino mixing Pontecorvo-Maki-Nakagawa-Sakata (PMNS) matrix U. Since the effective Majorana mass $\langle m_{ee}\rangle$ can be written in term of the

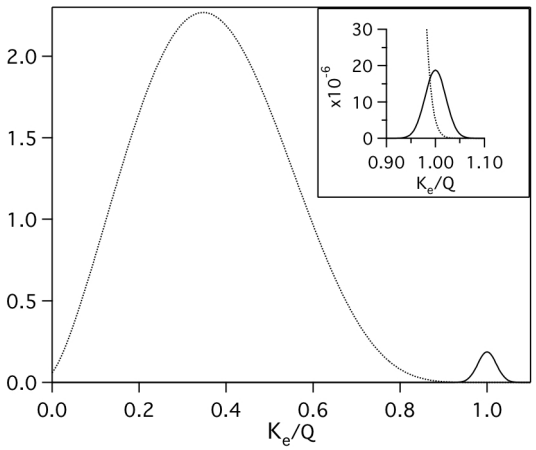

Figure 2. Energy spectra of the sum of the two electrons kinetic energies, normalized to the endpoint $Q_{\beta\beta}$. The $\beta\beta0\nu$ energy line is broadened by the limited energy resolution of the detector.

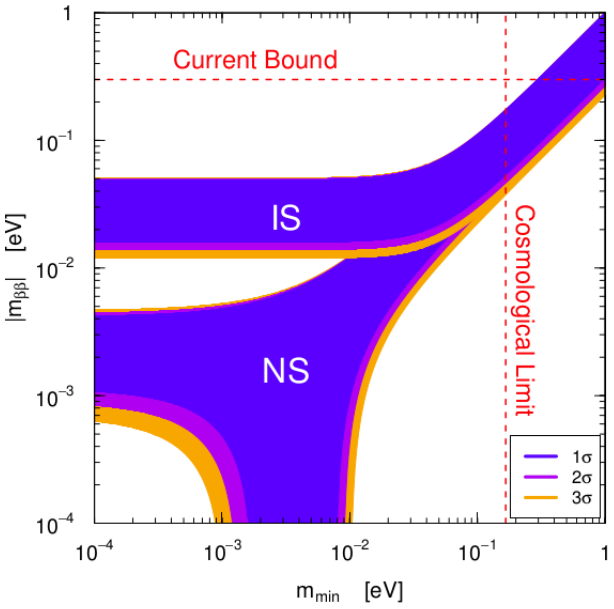

Figure 3. Value of the effective Majorana mass as a function of the lightest neutrino mass in the normal (NS) and inverted (IS) neutrino mass spectra (from [8]).

neutrino oscillation parameters, the results of the neutrino oscillation measurements can provide constraints on $\langle m_{ee} \rangle$ as a function of the neutrino mass scale. Figure 3 shows the predicted value of $\langle m_{ee} \rangle$ as a function of the smallest mass of neutrinos m_{min} [8]. The constraints depend on the neutrino mass pattern. We emphasis that these constraints are valid only for the standard $\beta\beta0\nu$ mechanism with the exchange of a virtual light Majorana neutrino. As previously discussed, other mechanisms can also contribute and thus can increase (positive interferences) or decrease (negative interferences) the $\beta\beta0\nu$-decay rate.

Theoretical uncertainties for the nuclear matrix element (NME) calculations are the main limitation in making interpretation of $\beta\beta0\nu$-decay or in comparing the sensitivity between

Isotope	$Q_{\beta\beta}$ (MeV)	$T^{2\nu}_{1/2}$ (yr)	$T^{0\nu}_{1/2}$ (yr) (90% C.L.)	$\langle m_{ee}\rangle$ (eV) Min.	Max.	Experiment (for 0ν limit)
^{48}Ca	4.274	$4.2^{+2.1}_{-1.0}\ 10^{19}$	$>$ 5.8 10^{22}	3.55	9.91	CANDLES [10]
^{76}Ge	2.039	$1.8\ ^{+0.14}_{-0.10} 10^{21}$	$>$ 2.1 10^{25}	0.20	0.50	GERDA [11]
^{82}Se	2.996	$9.0 \pm 0.7\ 10^{19}$	$>$ 3.2 10^{23}	0.85	2.08	NEMO-3 [12]
^{96}Zr	3.348	$2.0 \pm 0.3\ 10^{19}$	$>$ 9.2 10^{21}	3.97	14.39	NEMO-3 [13]
^{100}Mo	3.035	$7.1 \pm 0.4\ 10^{18}$	$>$ 1.0 10^{24}	0.30	0.78	NEMO-3 [12]
^{116}Cd	2.809	$3.0 \pm 0.2\ 10^{19}$	$>$ 1.7 10^{23}	1.22	2.30	SOLOTVINO [14]
^{130}Te	2.530	$0.7 \pm 0.1\ 10^{21}$	$>$ 2.8 10^{24}	0.27	0.57	CUORICINO [15]
^{136}Xe	2.462	$2.38 \pm 0.14\ 10^{21}$	$>$ 1.9 10^{25}	0.14	0.33	KamLAND-Zen [16]
		$2.23 \pm 0.22\ 10^{21}$	$>$ 1.6 10^{25}	0.15	0.36	EXO-200 [17]
^{150}Nd	3.367	$7.8 \pm 0.7\ 10^{18}$	$>$ 1.8 10^{22}	2.35	8.65	NEMO-3 [18]

Table 1. $\beta\beta2\nu$ half-life values and $\beta\beta0\nu$ half-life limits measured in a variety of experiments. Last two rows show the minimal and maximal upper limits on the effective majorana neutrino mass $\langle m_{ee}\rangle$, using NME's from [9].

different experiments measuring different isotopes. Depending on the theoretical models, NME's can vary by a factor 2 to 3. It results to a factor of uncertainty of about 4 to 10 on the required sensitivity to $T^{0\nu}_{1/2}$ or on the required mass of isotope, when we compare different experiments using different isotopes. A complete compilation of the most recent NME calculations have been recently proposed in [9]. This compilation will be used in the following.

Table 1 and Figure 4 give the current experimental limits on the $\beta\beta0\nu$ half-life $T^{0\nu}_{1/2}$, obtained with various experiments, and the corresponding lower and upper limits on the effective Majorana mass.

3. General remarks on the experimental aspects

In case of no signal, the half-life sensitivity for a $\beta\beta0\nu$ experiment is given by:

$$T^{0\nu}_{1/2} > \ln 2 \frac{\mathcal{N} M \varepsilon}{A} \frac{T_{obs}}{N_{excl}}$$

where M is the mass of enriched isotope, A its atomic mass, $\mathcal{N}$ the Avogadro, ε the $\beta\beta0\nu$ efficiency of the detector, T_{obs} is the duration of the measurement and N_{excl} is the number of excluded $\beta\beta0\nu$ events. From this relation, it is clear that the essential requirement of the double beta experiments is to achieve an extremely low radioactive background, a large mass of isotopes and a large detection efficiency. It is also important to note that in the case of no background, the half-life sensitivity increases as the duration of observation T_{obs}, while in the case of relatively larger background, it increases only as $\sqrt{T_{obs}}$.

There are several sources of backgrounds relevant to the $\beta\beta0\nu$ search and their issues depend on the experimental technique and isotope. The irreducible background comes from the energy tail of the standard $\beta\beta2\nu$ decay. It requires to have a high energy resolution and/or to measure a $\beta\beta$ isotope with a large $\beta\beta0\nu$ half-life. The second source of backgrounds comes from the decays of ^{214}Bi and ^{208}Tl originating from the natural decay chains of ^{238}U and ^{232}Th. ^{214}Bi is a β emitter with a high transition energy $Q_\beta \approx 3.2$ MeV, above the $Q_{\beta\beta}$ of most of the $\beta\beta$ isotopes. ^{208}Tl is the natural isotope with the highest energy transition (≈ 5 MeV): it is a β emitter ($Q_\beta \approx 2.4$ MeV) followed always by a γ emission with an energy $E_\gamma = 2.6$ MeV. The choice of $\beta\beta$ isotopes with a $Q_{\beta\beta}$ above 2.6 MeV allows to reduce strongly the background produced by the 2.6 MeV γ-ray. The ^{214}Bi and ^{208}Tl contaminations can also result from Radon

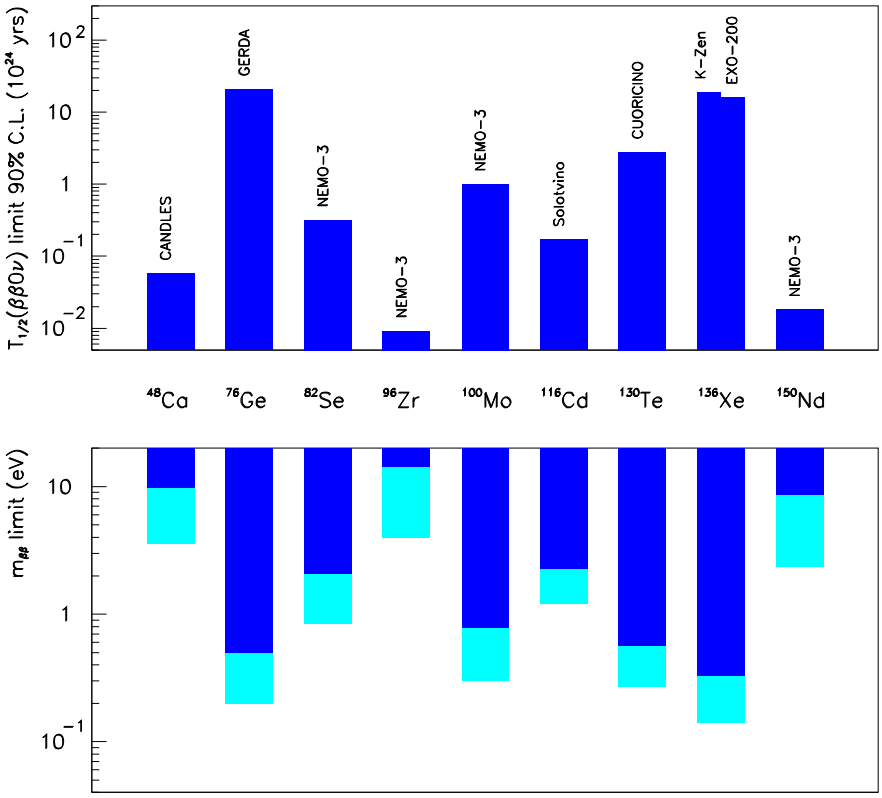

Figure 4. Current $\beta\beta0\nu$ half-life limits (90% C.L.) obtained in a variety of experiments (upper figure) and corresponding minimal and maximal upper limits on the effective majorana neutrino mass $\langle m_{ee}\rangle$, using NME's from [9] (lower figure).

(^{222}Rn) or Thoron (^{220}Rn) contamination. Radon and Thoron are a gas also originating from the natural decay chains of ^{238}U and ^{232}Th, which can diffuse inside the detector or emanate from materials. The Thoron contamination is generaly much lower than Radon due to its short half-life which limits its diffusion capacity. Another source of backgrounds comes from alpha's particles produced from ^{238}U and ^{232}Th contamination. If their energy is degraded before reaching the detector, they can pollute the $\beta\beta0\nu$ energy region. External high energy gamma's produced either by external neutrons or high energy cosmic muons can also produce $\beta\beta0\nu$ background. It requires to operate the detector in a underground laboratory and inside a low radioactive gamma and neutron shield. Cosmogenic is a critical background especially for calorimetric experiments with large mass of isotopes. Cosmogenics are long-lived cosmic ray induced isotopes produced during the $\beta\beta$ isotope enrichment process or during the detector fabrication above ground. Some cosmogenics are well known, like ^{60}Co ($T_{1/2} = 5.272$ years) or ^{68}Ge ($T_{1/2} = 270$ days) (for Germanium detectors). Others are not well known. This is the case for Xenon and could be a new background for future Xenon experiments. Finally contamination in rare natural or artificial isotopes can produce an unexpected background. As discussed in the next sections, the ^{42}K contamination in the liquid argon in GERDA experiment, and the

contaminants from Fukushima fallout (and possibly from other origins) in KAMLAND-Zen experiment are two examples.

A large variety of experimental techniques have been developed for the search of $\beta\beta0\nu$ decay. There are basically two types of experimental approaches: the calorimetric and the tracko-calo methods. In the calorimetric technique, the source is embedded in the detector itself which provides a high detection efficiency. With a proper choice of detector, a very high energy resolution up to FWHM=0.1% at $Q_{\beta\beta}$ can be achieved as in Germanium or bolometer detectors. However the capacity to prove that the observation is indeed a $\beta\beta0\nu$-decay, and not an unidentified background or an unknown gamma transition, is limited. Therefore the search of $\beta\beta0\nu$-decay requires several experimental techniques and more than one isotope. Recently large existing liquid scintillator detectors, initially developed for neutrino oscillation measurements (KamLAND, SNO), have been reused as $\beta\beta$ detectors by adding isotope inside the liquide scintillator. It allows to reach quickly a large amount of isotope ($\approx$ 100 kg) but with a limited energy resolution and thus a non negligible background. The tracko-calo method separates the detector from the source by the combination of a calorimeter and a tracking detector. It allows to reconstruct directly the track of each of the two emitted electrons from the source foil and also to identify and measure each background component. However the price is a lower $\beta\beta0\nu$ efficiency and a lower energy resolution. It is the most sensitive technique for the search of the $\beta\beta0\nu$ with V+A right-handed weak current, since it provides the angular distribution between the two emitted electrons.

In the next sections, the different techniques and projects will be reviewed: the germanium diodes, the bolometers, the large liquid scintillators, the Xenon TPC, the crystals at room temperature, and finally the tracko-calo detectors.

4. Germanium detectors

Ultra radiopure Germanium semiconductor diodes have been used historically as one of the first detectors for the direct search of $\beta\beta$-decay using source as detector [19]. The ^{76}Ge $\beta\beta$ emitter has unfortunately a relatively low transition energy $Q_{\beta\beta}$ = 2039 keV. Therefore germanium experiments are very sensitive to 2.6 Mev γ-rays from ^{208}Tl, to standard cosmogenics like ^{60}Co ($T_{1/2}$ = 5.272 years) and ^{68}Ge ($T_{1/2}$ = 270 days), and other possible contaminations like ^{42}K. However Germanium detectors are today well established detectors, manufactured in large amount, and excellent energy resolution of few keV at 2 MeV is obtained when diodes are used at Liquid Nitrogen temperature. Also recent development of Broad-Energy Germanium detectors provides superior pulse shape discrimination performances. It allows to suppress partially the γ's background (mainly multi-Compton interactions corresponding to multi-sites events), and to conserve the $\beta\beta$ events (single-site events).

In the 1990's, two experiments named Heidelberg-Moscou (HM) [20] in Gran Sasso Underground Laboratory (LNGS, Italy) and IGEX [21] in Canfranc Underground Laboratory (LSC, Spain) measured around 10 kg of enriched Ge^{76} and set a limit of about 1.510^{25} y on $T^{0\nu}_{1/2}(Se^{76})$ with a level of background of $\approx$ 0.2 cts/(keV.kg.y) and an energy resolution of $\approx$ 3 keV in the $\beta\beta0\nu$ energy region.

4.1. The GERDA experiment

In 2011, a new Germanium experiment, named GERDA [22], have started taking data in LNGS. It consists of using bare Germanium detectors directly immersed inside Liquid Argon which acts both as cryogenic liquid and shield against external γ's (Figure 5). Moroever, the detection of the scintillation light emitted in Argon can be used as an active shield against external γ's. The cryostat, with an inner diameter of 4 m, and a total height of $\approx$ 4 m, contains about 100 tons of liquid Argon. It is installed inside a larger water tank (diam=10m, height=8.5m) for extra γ and neutrons shield. The Ge detector array is made up of individual detector strings in the

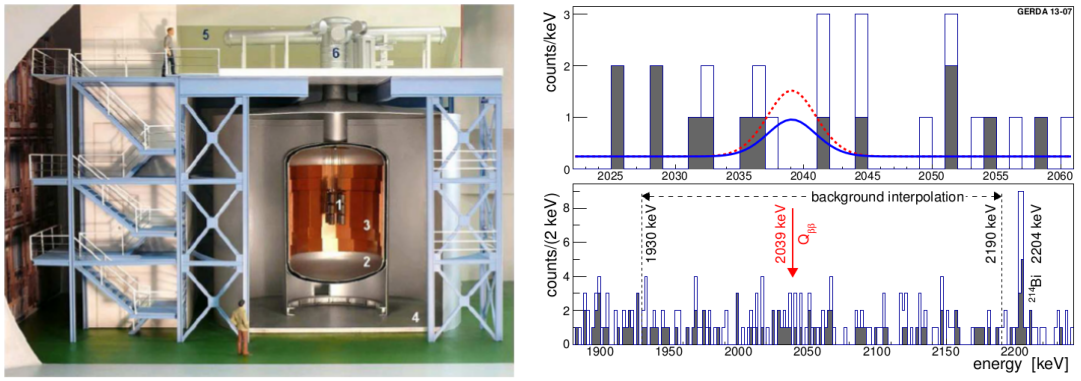

Figure 5. (Left) Schematic view of the GERDA experiment: (Right) Result of GERDA Phase 1, after 492.3 days of data collection and an exposure of 21.6 kg.yr of ^{76}Ge: energy spectrum without (open histogram) and with (filled histogram) pulse shape discrimination (from [11]). The limit (90% C.L.) obtained on the $\beta\beta0\nu$ signal with the extrapolated expected background are superimposed (blue line). The lower panel shows the region used for the flat background interpolation.

central part of the cryostat. This strings design allows to deploy crystals progressively inside the experiment.

Results from the GERDA first phase of data collected until May 2013 (492.3 live days) have been recently reported in [11] (Figure 5). It uses 8 refurnished Ge crystals from previous HM and IGEX experiments, and 5 newly produced enriched BEGe detectors, corresponding to about 21 kg of enriched ^{76}Ge. The corresponding total exposure is 21.6 kg.y of Ge, and a $\beta\beta0\nu$ efficiency of about 70%. The averaged energy resolution (FWHM), extrapolated at $Q_{\beta\beta}$, is about 5 keV for refurnished detectors and about 3 keV for new BEGe detectors. No excess of signal has been observed at $Q_{\beta\beta} \pm 5$ keV, resulting to a lower limit for the $\beta\beta0\nu$ half-life for ^{76}Ge of $T_{1/2}(\beta\beta0\nu) > 2.1\ 10^{25}$ y (90% C.L.). The measurement of the $\beta\beta2\nu$ decay have been also measured [23] with a half-life of $T_{1/2}(\beta\beta2\nu) = \left(1.8\ ^{+0.14}_{-0.10}\right)\ 10^{21}$ y

The initial measurements showed a prominent and unexpected background due to the drift of the positively charged ^{42}K on the germanium diodes. In order to reduce this background, copper electrostatic shields surrounding the detector arrays have been installed. The observed background, in the $\beta\beta0\nu$ energy region, is now without pulse shape analysis $1.8 \pm 0.2\ 10^{-2}$ cts/(keVkgyr) for semi-coaxial detectors and $4.2 \pm 1.\ 10^{-2}$ cts/(keVkgyr) for BEGe detectors. After pulse shape discrimination, the observed background becomes $1.1 \pm 0.2\ 10^{-2}$ cts/(keVkgyr) for semi-coaxial detectors and $0.5 \pm 0.4\ 10^{-2}$ cts/(keVkgyr) for BEGe detectors, it means an order of magnitude lower than in previous experiments. A single dominant contribution to the background at $Q_{\beta\beta}$ cannot be identified and its understanding and exact location is statistically limited and will require longer measurements. The origins of background modelized in simulation are Compton electrons from γ-rays of ^{208}Tl and ^{214}Bi decays, β decays from ^{42}K (the progeny of ^{42}Ar) and ^{214}Bi close to or on the surface of the detector, and degraded α's from contaminations on the surface of the detectors.

In the second phase of data, new BEGe detectors containing 35 kg of enriched germanium will be installed. Adding the 18 kg of Phase 1, GERDA Phase II will measure up to ≈ 50 kg of enriched ^{76}Ge. The goal is to reach a level of background of 0.001 cts/(keV.kg.y), an order of magnitude lower than the observed one in Phase I. It will lead to a sensitivity of $\approx 2.\ 10^{26}$y in 2 years of measurement. In order to reach this level of background, the detection of the scintillation light from argon will be installed as veto of external γ background (as demonstrated

by the LArGe prototype). Also efforts of surface radiopurities of the BEGe detectors must be ensured for the production of the next detectors in order to reduce background produced by β-decay or degraded α from potential surface contaminations.

Depending of the achieved background, extra enriched germanium detectors could be produced and installed inside GERDA for a third phase. The goal is to reach a sensitivity of $\approx 10^{27}$y with 100 kg of enriched Ge and 10 years of measurement, with a background lower than 0.001 cts/(keV.kg.y).

4.2. The MAJORANA experiment

Another germanium experiment, named MAJORANA experiment, is under development in the USA and will be located in the Sanford Underground Laboratory (USA). In contrast with GERDA, the germanium detectors are runned in vacuum Nitrogen cryostat with standard low-background passive lead and copper shield and an active muon veto. A total of 70 BEGe detectors will be measured with the demonstrator corresponding to 30 kg of 86% enriched Ge and 10 kg of natural germanium crystals. Two independent cryostats will be constructed using ultra-clean and underground electroformed copper (the electroforming will be performed underground). The experiment should start in 2014.

Possible limitations of the next generation of experiments measuring a ton of germanium have been studied in [24]. The usual contamination in ^{210}Pb, observed on the crystal surface, produces a limiting background from degraded α's. To illustrate, 100 of ^{210}Pb nuclei per m^2 would produce $\approx 10^{-5}$ counts/(kg.y.keV) in the $\beta\beta0\nu$ energy region. The ^{210}Pb screening methods and clean solvents ($< 10\mu$Bq/m^3) are needed. The bulk contamination of the germanium crystals in ^{68}Ge cosmogenic isotope ($T_{1/2} = 3.84$ years) is also a limiting background [25]. Next generation experiment requires R&D on deenrichment of ^{68}Ge with a deenrichment factor of at least 2 10^{-5} to get less than 0.5 ^{68}Ge nucleus per kg, corresponding to a background of 10^{-5} counts/(kg.y.keV).

5. Bolometer detectors

5.1. Standard $Te0_2$ bolometers: the CUORE experiment

The use of bolometers for $\beta\beta0\nu$-decay searches was suggested by Fiorini and Niinikoski in 1984 [26] and applied first by the Milano group in the MIBETA experiment [27] using natural $Te0_2$ crystals as bolometers.

The main advantage to use $Te0_2$ crystal is that the natural abundance of ^{130}Te (the $\beta\beta$ emitter) in tellerium is high, about 34 %. However its $Q_{\beta\beta} = 2530.3 \pm 2.0$ keV is lower than the 2615 keV γ ray from ^{208}Tl. Experiments using TeO_2 crystals are therefore sensitive to Compton electron background due to any ^{232}Th contamination.

In the 2000's, an experiment named CUORICINO and located in LNGS, measured a total mass of 40.7 kg of TeO_2, corresponding to a total mass of 11.6 kg ^{130}Te isotope. The detector contained 62 TeO_2 crystals ($5 \times 5 \times 5$ cm^3) assembled inside a tower of about 1 m height. The average energy resolution (FWHM) was 7 keV at $Q_{\beta\beta}$ and the $\beta\beta0\nu$ detection efficiency was 0.83%. No excess of events had been observed at $Q_{\beta\beta}$, resulting to a limit on the $\beta\beta0\nu$-decay half-life of $T_{1/2}(\beta\beta0\nu) > 2.8\ 10^{24}$ yrs (90% C.L.) [15].

The background in the $\beta\beta0\nu$ energy region was measured to be 0.17 cts/(keV.kg.y). The two origins of the backgrounds are (i) external 2615 keV γ-ray from ^{208}Tl (^{232}Th) contaminations, mostly in the cryostat and the external shield, and (ii) degraded α's from ^{238}U and ^{232}Th surface contamination mostly from copper surrounding the crystals.

CUORICINO was a pilot detector for a larger experiment, named CUORE, currently in construction, which will measure up to 200 kg of ^{130}Te. The CUORE experiment [28] consists of an array of 988 TeO_2 $5 \times 5 \times 5$ cm^3 crystals, assembled in 19 individual towers and operating at 10 mK in a new large cryostat with improved external shield (see Figure 6). The goal is

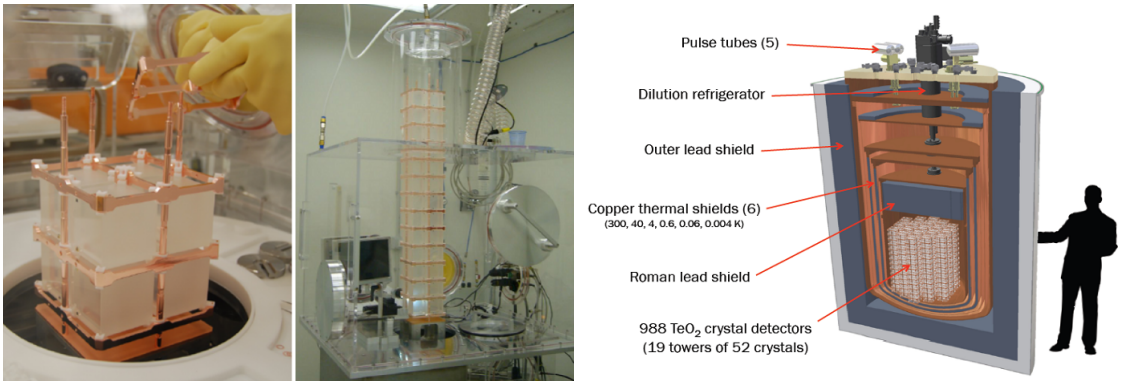

Figure 6. (Left) Photos of the assembly of the TeO_2 crystals and of the first CUORE-0 tower; (Right) Schematic view of the full CUORE experiment with the 19 bolometer towers installed in a unique large cryostat with low radioactive shield.

to reach a level of background of 0.01 cts/(keV.kg.yr), an order of magnitude lower than in CUORICINO. It will correspond to an expected sensitivity of $T_{1/2}(\beta\beta0\nu) > 10^{26}$ yrs (90% C.L.) after 5 years of measurement with the complete CUORE detector.

The first tower, named CUORE-0 (see Figure 6), is currently taking data in the old Cuoricino cryostat since March 2013. The preliminary energy resolution (FWHM) is 5.6 keV (FWHM) at $Q_{\beta\beta}$ value. After 7 kg.yr of exposure, the background index in the $\beta\beta0\nu$ energy region is 0.074 ± 0.012 cts/(keV.kg.yr) [29]. It is a factor two lower than in CUORICINO. The α contribution has been reduced by a factor 6. The rest of the backrgound, observed in the $\beta\beta0\nu$ energy region, is dominated by the external γ from the CUORICINO cryostat and shield. A higher radiopurity cryostat facility and a higher shield efficiency is expected for CUORE, in order to reduce the external γ backrgound. It will have to be demonstrated with the first data with the final CUORE cryostat.

5.2. Scintillating bolometers: the LUMINEU and LUCIFER experiments

The scintillating bolometers, based on scintillating crystals, allows the simultaneous detection of heat and scintillation light. It allows the suppression of the background due to degraded α particles, thanks to the different scintillation quenching factor between α and β/γ. Moroever, with a crystal based on a double beta isotope with a $Q_{\beta\beta}$ transition value above the 2615 keV ^{208}Tl γ-line, the external γ background is strongly suppressed. Thus scintillating bolometers appear to be a very promising calorimetric technique to suppress the current background observed in standard TeO_2 bolometers.

$CdWO_4$ (^{116}Cd, $Q_{\beta\beta} = 2809$ keV) was the first scintillating crystal studied for $\beta\beta0\nu$ search. However, no project has been proposed, due to the relative high cost for ^{116}Cd enrichment.

The LUMINEU project [30] proposes to use $Zn^{100}MoO_4$ crystals (^{100}Mo, $Q_{\beta\beta} = 3034$ keV). A first large 330 g $ZnMoO_4$ crystal, produced in Novosibirsk (Russia), has been successfully tested in LNGS [31]. The bolometer has shown a good energy resolution of about 6 keV (FWHM) at the 2615 keV γ line of ^{208}Tl and an excellent discrimination between α and β/γ events (see Figure 7). It has been also observed that the pulse shape discrimination of the phonon (heat) signal alone, is sufficient to discriminate β/γ to α particles [32][33]. Moroever, this crystal shows an excellent radiopurity (less than 6 μBq/kg in ^{228}Th and 27 ± 6 μBq/kg in ^{226}Ra). New large crystals have been recently produced and are under test. Assuming the CUORICINO cryostat equipped with ZnMoO4 crystals (≈ 30 kg of crystal and 13 kg of ^{100}Mo), and a typical energy resolution of FWHM= 5 keV, the expected background is few 10^{-4} cts/(keV.kg.y) and

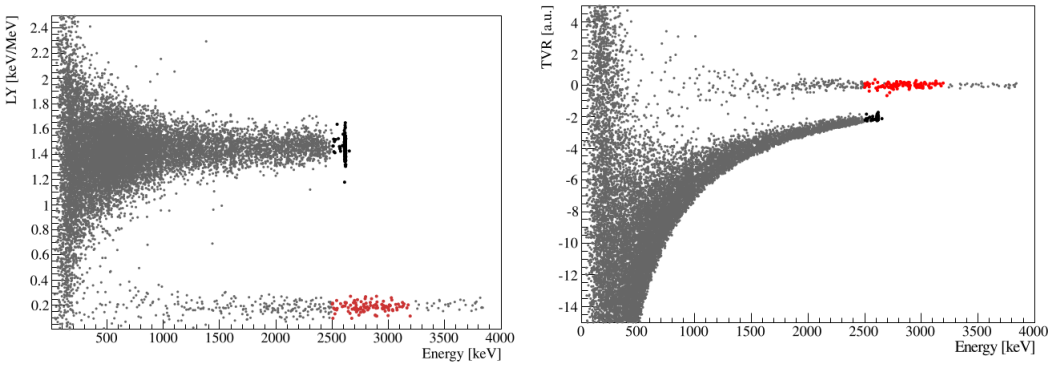

Figure 7. Large $ZnMoO_4$ crystal exposed to a ^{228}Th source. (Left) The light-to-heat energy ratio as a function of the heat energy: the β/γ events (upper band) and α events (lower band) are clearly separated; (Right) TVR parameter (see text) as a function of the energy, for the same events (from [31]).

the expected sensitivity is about 10^{26} yrs in 5 years of running. For larger isotope mass, developments of new NTD readout, delivering faster phonon signal, are required in order to suppress the background from the pile-up of two successive $\beta\beta2\nu$ decays. Today about 10 kg of enriched ^{100}Mo is available (isotope used in the old NEMO-3 experiment) and can be used in LUMINEU experiment.

The LUCIFER experiment uses ZnSe crystals (^{82}Se, $Q_{\beta\beta} = 2995$ keV) because of its large light yield and its relatively low cost to enrich ^{82}Se. The goal is to build a demonstrator with few tens of kg of enriched $Zn^{82}Se$ and to reach a level of background of 10^{-3} cts/(keV.kg.yr). The design of the LUCIFER experiment is similar to CUORICINO. It consists of a tower of 12 modules, each elementary module corresponds to an array of 4 ZnSe crystals (each crystal $5\times5\times5$ cm^3, 660 g) read out by a single light detector. The setup could house up to ≈ 20 kg of ^{82}Se isotope corresponding to an expected sensitivity of $\approx 10^{26}$ yrs after 5 years of running and a level of background of 10^{-3} cts/(keV.kg.yr). Experimental studies of several ZnSe crystals as scintillating bolometers have been performed in the last few years [34]. A relatively large light yield and good energy resolution have been obtained. However an unexpected characteristic has been observed with ZnSe: the scintillation light yield for α is larger than for β/γ of the same energy. When the α band is spread to lower light signal, α particles can then be misidentified as β/γ events. Today the main issue of the LUCIFER experiment is the production of pure ZnSe crystals without metallic contaminations in order to obtain good heat and light performances and good reproducibility of the crystals growing.

If these pilot experiments reach the required level of background, the scintillating bolometer technique can be extended to larger scale. For instance, 19 towers equipped with enriched $Zn^{100}MoO_4$ crystals and installed in the CUORE cryostat (corresponding to 230 kg of ^{100}Mo), and a level of background of 10^{-3} cts/(keV.kg.yr) (or about 2.5 cts/(FWHM.yr)) would give a sensitivity for the $\beta\beta0\nu$ search of about $\approx 10^{27}$ yrs after 5 years of running, corresponding to a limit on the effective Majorana neutrino mass of $\langle m_{ee}\rangle < 10 - 30$ meV.

6. Large liquid scintillators detectors

Recently two large existing liquid scintillator detectors, KamLAND and SNO, initially developed for neutrino oscillation measurements, have been reused as $\beta\beta$ detectors by adding $\beta\beta$ isotope inside the liquide scintillator. It allows to reach relatively quickly a large amount of isotope.

6.1. The KamLAND experiment

The KamLAND-Zen experiment, currently running in the Kamioka mine (Japan), measures ^{136}Xe isotope. There are three advantages to use^{136}Xe: it is the simplest and least costly $\beta\beta$ isotope to enrich, its high $\beta\beta2\nu$ half-life ($\simeq 2\ 10^{21}$ y) reduces naturally the $\beta\beta2\nu$ background, and it is relatively easy to dissolve Xenon gas in liquid scintillator with a mass fraction of a few % [35]. KamLAND [36] consists of a sphere (13 m diameter) filled with ultra radiopure liquid scintillator ($0.2 - 2\ 10^{-18}$ g/g in ^{238}U and $1.9 - 4.8\ 10^{-17}$ g/g in ^{232}Th), contained in a second sphere filled of inert buffer oil (shield), surrounded by a water Cerenkov outer detector. The major modification of KamLAND-Zen [16] to the KamLAND experiment was the installation of an inner, very radiopure , very thin (25μm) and very transparent balloon (≈ 3.1 m diameter), suspended at the center of the KamLAND detector (see Figure 8. This ballon contains 13 tons of Xe-loaded liquid scintillator (Xe-LS) with 2.5% of Xenon dilution, equivalent to 300 kg of ^{136}Xe. The energy resolution is $\approx$ 10% (FWHM) at $Q_{\beta\beta}(^{136}Xe)$. The external liquid scintillator acts as an active shield against external γ's. In order to reduce the background from the ballon material, the reconstructed vertex of events must be within 1.35 m of the ballon center, defining a fiducial volume of 62 % of the total volume, with an effective mass of ^{136}Xe of 179 kg. Results of the first phase of the KamLAND-Zen experiment (Oct. 2011 to June 2012, 213.4 days of data and an exposure of 89.5 kg.yr of ^{136}Xe) have been recently published [16]. Figure 8 shows the energy spectrum of selected $\beta\beta$ events, with the best fitted background. The $\beta\beta2\nu$-decay signal is well observed and measured. However an unexpected background has been observed in the $\beta\beta0\nu$ energy region, with a strong peak near the Q-value of the $\beta\beta$ decay. This background comes from ^{110m}Ag contamination ($T_{1/2} = 360$ days, $Q_\beta = 3.01$ MeV). It is a fission product, which has probably contaminated the detectors materials by fallout from the Fukushima reactors accident Assuming this ^{110m}Ag contamination, a limit to the half-life of the $\beta\beta0\nu$ decay has beed derived: $T^{\beta\beta0\nu}_{1/2}(^{136}\mathrm{Xe}) > 1.9\ 10^{25}$ yrs (90% C.L.). In order to study the origin of the ^{110m}Ag observed background, Xe-LS has been filtered then Xe has been extracted and distilled and finally LS has been purified several times. A reduction of the ^{110m}Ag by a factor 3 to 4 has been measured after one LS purification pass. The collaboration plan to restart taking data after several volume purifications. A new mini-ballon might be also produced if the ^{110m}Ag background is still too high. The collaboration plans also to load up to 600 kg of enriched ^{136}Xe, already available. In a second phase in 2016, up to 1 ton of ^{136}Xe might be loaded, after increasing the PMT coverage from 24% up to 70% with Winston cone reflectors and by increasing the Xe-LS light yield.

The preliminary result obtained by KamLAND-ZEN illustrates an important feature: a pure calorimeter detector with a relatively modest energy resolution (FWHM of few percent at $Q_{\beta\beta}$) is a well detector to reach a high sensitivity in case of no background, but cannot distinguish a possible signal to a mimicking γ emitter background in case of possible contamination. A possible risk of contamination of the xenon itself has to be also considered for next measurements. Cosmic activation of Xenon is not well known and can be a source of background. But the most critical background with ^{136}Xe comes from the rare 2447 keV γ-ray (intensity 1.57%) emitted by ^{214}Bi. When the γ is totally contained, it produces a peak very close to the expected $\beta\beta0\nu$ signal at $Q_{\beta\beta} = 2462$ keV.

6.2. The SNO+ experiment

SNO+ [38], currently in preparation, proposes to fill the Sudbury Neutrino Observatory (SNO) with ultrapure natural Te-loaded liquid scintillator, in order to investigate the isotope ^{130}Te. The measured light yield of load-Te liquid scintillator is high with no absorption lines, which gives a potential to increase the Te loading concentration. The expected $\beta\beta2\nu$ background is very low thanks to the high $\beta\beta2\nu$ half life of ^{130}Te. However, due to the low $Q_{\beta\beta}$ value of ^{130}Te ($Q_{\beta\beta} = 2.53$ MeV), it requires a high radiopurity of the liquid scintillator in ^{238}U and

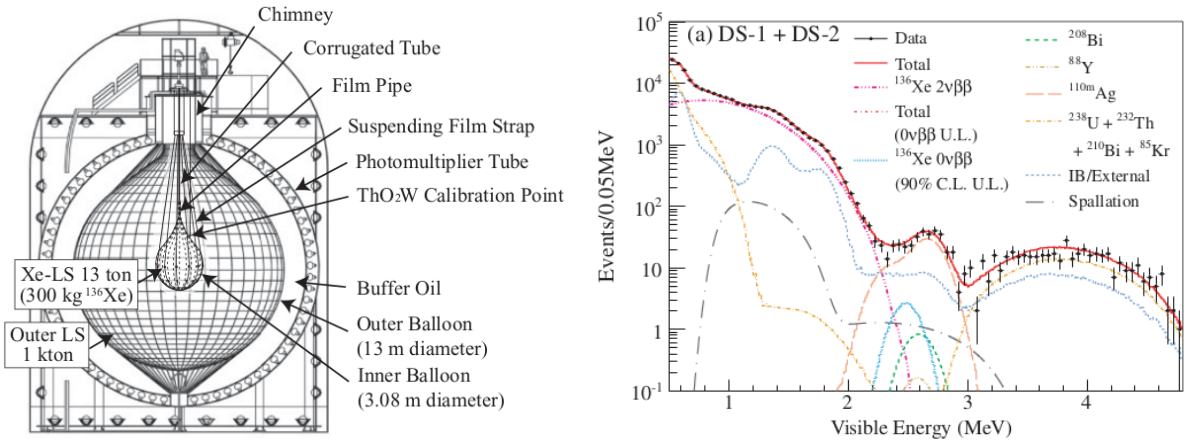

Figure 8. (Left) Schematic view of the Kamland-Zen detector (from [37]; (Right) Result of KamLAND-Zen after 213.4 days of data collection and an exposure of 89.5 kg.yr of ^{136}Xe: energy spectrum of selected $\beta\beta$-decay candidates together with the best-fit backgrounds and $\beta\beta2\nu$-decays, and the 90% C.L. upper limit for $\beta\beta0\nu$ process (from [16]).

^{232}Th and interface regions must be very tight against leak of external mine air to avoid Radon contamination. The present plan is to dilute 0.3% in mass of natural Te salt in 1 ktons of liquid scintillator, providing a source of 800 kg of enriched ^{130}Te, or 160 kg in a 3.5 m fiducial volume. The Te loading concentration will be increased once the the technique will be demonstrated.

Given the liquid scintillator light yield and photocathode coverage of the experiment, an energy resolution performance of about 8% FWHM at the $Q_{\beta\beta}$ value, is expected. External backgrounds can be rejected by the external water shielding, self-shielding of the scintillator and with a 20% fiducial volume selection. The crucial point is the radiopurity of the liquid scintillator. An extensive set of scintillator purification systems are under construction with the aim of reaching the purity levels (10^{-17} g/g of ^{238}U and ^{232}Th chain activities) achieved by the Borexino experiment. The internal ^{214}Bi and ^{208}Tl contamination in Xe-LS can be tagged and reduced by the delayed $\beta - \alpha$ coincidence. The expected rejection efficiencies are 99.99% and 97%, respectively. It is also proposed to differentiate α from β events by scintillator timing profiles. The cosmogenic background is expected to be reduced to negligible level, minimizing the isotope time at surface. The ultimate background are the ^{8}B solar neutrinos with an expected level of about 3 10^{-2} cts/year/keV. However this level of background remains constant when the percent of Te loading is increased. The total expected background in the FWHM energy window around the $Q_{\beta\beta}$ value is few tens of counts per year. SNO+ compensate this relatively large background (due to a modest low energy resolution) by a large mass of ^{130}Te. It is scheduled to start taking data with the acrylic vessel filled with pure water. The water will be then replaced by the purified liquid scintillator and data will be collected during few months. First data with ^{nat}Te-loaded scintillator are foreseen by the end of 2014. It is claimed that the initial 0.3% loading of Te is projected to reach the inverted hierarchy and increased loading to 3% could cover the inverted hierarchy.

A possible improvement for the next generation of liquid scintillator detectors would be the ability to reconstruct the direction of the events, providing a topology of the event,and therefore an increase of the background rejection efficiency. L. Winslow et al. [39] recently proposed to distinguish the directional Cerenkov light from the isotropic scintillation light in order to reconstruct the direction and the topology of the event.

7. Xenon TPC detectors

7.1. The EXO experiment

The EXO-200 detector [17] is a time projection chamber (TPC) using 200 kg of liquid Xenon (enriched at 80% in ^{136}Xe), and located in the Wast Isolation Pilot Plant (USA). It started taking data in 2011. The main advantage of a liquid TPC is its compact geometry. The TPC is a cylinder of 40 cm diameter and 44 cm length with a cathode grid dividing the cylinder into two identical regions. Each end of the TPC contains two wire grids and an array of 250 large-area avalanche photodiodes, that allows for simultaneous readout of ionization and scintillation in liquid xenon. Wire grids provide a 2-dimensional transversal localization and energy information while the third longitudinal coordinate is obtained from the scintillation light. The energy resolution is FWHM = 3.9% ($\approx$ 100 keV) at the $Q_{\beta\beta}$ value, using the anti-correlation between ionization and scintillation [40]. The ability of the TPC to reconstruct energy depositions in space is used to remove interactions at the detector edges where the background is higher. It reduces to a fiducial volume containing 80 kg of ^{136}Xe. It also provides a discrimination between single-cluster depositions (SS events), characteristic of $\beta\beta$ and single β decays in the bulk of the Xenon, from multi-cluster ones (MS events), generally due to γ-rays background.

The results of the first 120.7 days of data collected (Sept. 2011 to Apr. 2012), corresponding to an exposure of 32.5 kg.yr, are presented in Figure 9 [17]. The SS and MS energy spectra are simultaneously fit with the probability density functions (PDFs calculated by Monte Carlo) of the $\beta\beta2\nu$ and $\beta\beta0\nu$ of ^{136}Xe with PDFs of various backgrounds. The dominant background in the $\beta\beta0\nu$ energy region comes from the radon in the cryostat-lead air-gap and the ^{232}Th and ^{232}U in the TPC vessel. The radon and thoron contaminations inside the Liquid Xenon have been measured of 4.5 μBq/kg and $< 0.04\mu$Bq/kg respectively, corresponding to a negligible background. The $\beta\beta2\nu$-decay signal is well observed and measured in the SS spectrum. The level of background in the $\beta\beta0\nu$ energy region is measured to be $(1.5 \pm 0.1) \times 10^{-3}$ /(kg.keV.y), corresponding to about 12 counts per year in the FWHM energy window at $Q_{\beta\beta}$. No evidence for $\beta\beta0\nu$ decay has been found, corresponding to a limit on the $\beta\beta0\nu$ half life of $T^{0\nu}_{1/2} > 1.6\ 10^{25}$ yrs (90%C.L.) New result based on full data set from Sept. 2011 to June 2013, corresponding to a factor of 3.6 greater exposure than published result, should be delivered soon. The dominant background in the $\beta\beta0\nu$ energy region comes from the radon in the cryostat-lead air-gap and the ^{232}Th and ^{232}U in the TPC vessel. A radon trap facility is under construction in order to flush radon-free air inside the shield and thus suppress the radon background. Assuming this component of background reduced to a negligible level, the level of background is expected to be about 5 cts/(FWHM.yr).

The EXO collaboration is designing a multi ton EXO detector, named nEXO. It will measure 5 tons of 90% enriched ^{136}Xe. Assuming a slightly improved energy resolution of 3.5% (FWHM) at the $Q_{\beta\beta}$ value, a complete radon suppression and 10 years of measurement, the expected sensitivity would be $T^{0\nu}_{1/2} > 4\ 10^{27}$ yrs (90%C.L.). This calculation assumes that the background is dominated by ^{214}Bi deposition on the surface of the TPC (due to produced by the drift of polonium ions, progenity of Radon decay, inside the LXe) or ^{208}U and ^{238}Th contaminations in the materials surrounding the TPC. In this case, the background level scales as the surface of the TPC, while the number of Xe nuclei scales as the volume of the TPC.

7.2. The NEXT experiment

The NEXT-100 experiment [41], under construction in the Canfranc Underground Laboratory (LSC, Spain), proposes to use a gaseous Xe TPC, using the electroluminescence (EL) technique for the calorimetric TPC readout. The advantage of the NEXT concept is to provide an energy resolution better than 1% FWHM and a topological signal that can be used to reduce the background. The goal of the NEXT-100 detector is to demonstrate that this technology can be extrapolated to a 1-ton scale experiment with low background. The principle of NEXT-100 is

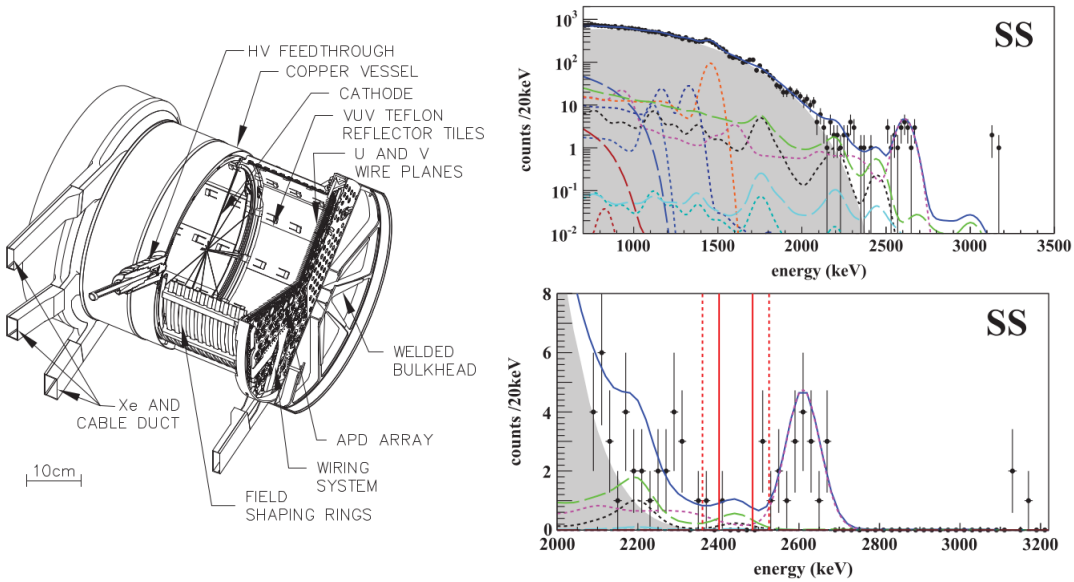

Figure 9. (Left) Schematic view of the EXO-200 liquid Xenon TPC; (Right) Result of EXO-200 after 120.7 days of data collection and an exposure of 32.5 kg.yr of ^{136}Xe: energy spectrum of selected $\beta\beta$-decay candidates (single-cluster events) together with the best-fit backgrounds and $\beta\beta2\nu$-decays (grey region). The dominant background in the $\beta\beta0\nu$ energy region (lower plot) comes from the radon in the cryostat-lead air-gap (long-dashed green) and the ^{232}Th and ^{232}U in the TPC vessel (dotted black and dotted magenta, respectively (from [17]).

as follows (Figure 10):

- The prompt primary scintillation light emission (in VUV) is detected via photodetectors (60 PMT's). This faint signal determines the t_0 time used for event position along the longitudinal drift.
- Then ionisation electrons drift toward the opposite anode (1 mm/μs, 0.5 kV/cm). The diffusion at 10 bar is about 9 mm/$\sqrt{\text{m}}$ transverse, and about 4 mm/$\sqrt{\text{m}}$ longitudinal.
- An additional grid in front of the anode creates 0.5 mm thick region of more intense field ($E/p \approx 4$ kV/cm/bar). A secondary scintillation light, named *electroluminescence*, is created in between grids by atomic desecitation, with very linear gain of order 10^3 and over a ≈ 2 μs interval. Finally, a segmented photodetector plane (7500 SiPM channels), located just behind the anode, performs the "tracking"
- The electroluminescence light, emitted isotropically, also reaches the cathode. The same array of PMT's used for t_0 measurement is also used for accurate calorimetry. A coating on the inner surface of the vessel improves the light collection.

In the NEXT-100 baseline design, the size of the field cage is 130 cm long, and 105 cm diameter, corresponding to a volume of $\simeq$1.1 m^3. The operation pressure ranges from 10 up to 15 bars. The NEXT-100 target is to reach an energy resolution better than 1% FWHM at $Q_{\beta\beta}$, a level of background of 2 10^{-4} cts/(keV.kg.yr) in the $\beta\beta0\nu$ energy region, with a $\beta\beta$ efficiency of 30% due to a $\beta\beta0\nu$ topological signature for background suppression.

A prototype, named NEXT-DEMO, has been developed to demonstrate both the energy resolution and the capability for tracking topology with two planes of photodetectors (PMT and SiPM) [42]. The drift region was 30 cm. An energy resolution of 1.8% FWHM at 511 keV have been obtained, corresponding to 0.8% FWHM at the $Q_{\beta\beta}$ value, better than the NEXT

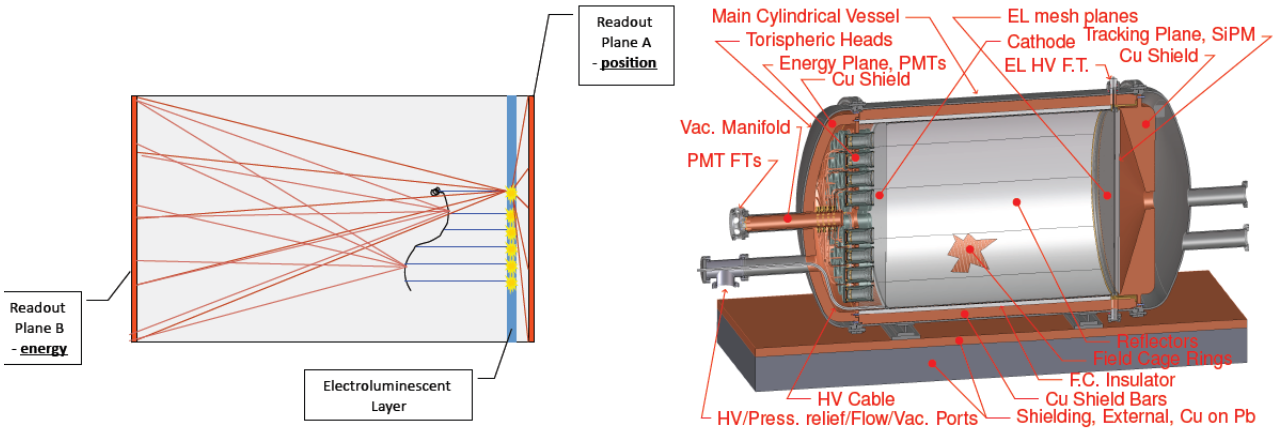

Figure 10. (Left) Principle of the electroluminescence TPC; (Right) Design of the NEXT-100 TPC (from [41]).

target of 1%. The first reconstructed tracks on the tracking SiPM panel show visible blobs at the extremity of the tracks for electron events produced by ^{22}Na and ^{137}Cs source. This preliminary result demonstrate the topology capabilities of the NEXT technology. However a complete analysis of the full collected events is still required in order to quantify the background rejection and $\beta\beta$ selection efficiency.

Recently, the NEXT collaboration decided to first assemble and test inside the NEXT-100 vessel, a smaller field cage (with dimensions reduced by a factor 2) with 10 kg of enriched ^{136}Xe and with 20% of the photodetectors (12 PMTs and 20 8×8 SiPM boards). Selection and construction of radiopure elements are in progress [43]. The goal of this first phase is to demonstrate the request background level and the topology capabilities.

8. Crystals at room temperature: CANDLES and COBRA experiments

CANDLES proposes to use natural CaF_2 crystals as scintillating detectors for the measurement of the isotope ^{48}Ca. The main advantage of ^{48}Ca is its high transition energy $Q_{\beta\beta} = 4274$ keV, well above the ^{208}Tl γ-ray (2.6 MeV), the ^{214}Bi β-decay (3.3 MeV end point), and α's from natural radioactivity (max. 2.5 MeV with scintillation quenching factor). Another advantage is its low atomic mass, providing a larger number of nuclei per mass unit. However, its natural abundance is very low, only 0.187% and it is today very difficult to enrich ^{48}Ca in large quantities. We mention that historically CaF_2 was one of the most sensitive technique used for the search of $\beta\beta0\nu$ [44].

CANDLES-III [45] is an array of 96 natural pure CaF_2 crystals ($10 \times 10 \times 10$ cm^3), for a total mass of $\approx$ 300 kg, corresponding to about 300 g of ^{48}Ca. Crystal are immersed inside a liquid scintillator as active veto and an external water buffer for an additional passive shield. The achieved energy resolution is $\approx$ 4.5% FWHM at $Q_{\beta\beta}$. The detector has been installed in the Kamiokande Underground Laboratory (Japan) and its commissioning has started in 2011.

There are two potential backgrounds, coming from ^{238}U and ^{232}Th contaminations inside the crystals or in the liquid scintillator in the vicinity of the crystals: the (β + delay α) pile-up events from ^{212}Bi-^{212}Po (β up to 2.2 MeV and quench $\alpha \approx 2.5$ Mev) and ^{214}Bi-^{214}Po cascades, and the ($\beta + \gamma$) pile-up events from ^{208}Tl decay (β up to 2.6 MeV and γ 2.6 MeV). The crystals and the liquid scintillator must be ultra radiopure: the average radiopurities of the crystals are $\approx$ 36 μBq/kg and $\approx$ 28 μBq/kg in ^{238}U and ^{232}Th chains, respectively. Residual BiPo β+delayα pile-up events are identified using pulse shape analysis with a rejection

efficiency of $\approx 90\%$ [10]. $\beta + \gamma$ pile-up events are the dominant background. Despite a modest energy resolution, the $\beta\beta2\nu$ background is negligible, about 0.01 counts per year. The total expected level of background in the $\beta\beta0\nu$ energy region (estimated by Monte-Carlo) is about 10^{-3} cts/(FWHM.kg.yr), equivalent to about 0.3 counts per year [45]. It corresponds to an expected sensitivity of $T^{0\nu}_{1/2} > 3.7\ 10^{24}$ yrs (90% C.L.) with 5 years of collected data.

We also mention the COBRA [46] project witch proposes to use an array of ^{116}Cd-enriched CdZnTe semiconductor detectors at room temperature. Small scale prototypes have been realized at LNGS (Italy). The proved energy resolution is 1.9% FWHM. The project is in R&D phase. Recent results on pixellization shows that the COBRA approach may allow an excellent tracking capability, equivalent to a solid state TPC.

9. Tracko-Calo detectors

In the NEMO detectors, also called tracko-calo detectors, the $\beta\beta$ sources are in the form of very thin and large foils and are separated from the detector. The combination of a tracking detector and a calorimeter provides both the measurement of the $\beta\beta$ energy spectrum and the direct reconstruction of the tracks of the two emitted electrons from the source foil (see Figure 11) . The efficiency to reject the background is therefore very high and any unknown γ line can be identified and rejected. However the energy resolution and the efficiency to detect a possible $\beta\beta0\nu$ signal are relatively low compared to pure calorimetric detectors. Moreover the size of the detector must be relatively large in order to contain a large mass of $\beta\beta$ source foils.

9.1. The NEMO-3 experiment

The NEMO-3 experiment took data in the Modane underground laboratory (LSM, France) from 2003 to 2010 and measured several double beta isotopes for a total mass of ≈ 10 kg. The two main isotopes for the $\beta\beta0\nu$ search were ^{100}Mo (35 kg.y of exposure) and ^{82}Se (4.5 kg.y of exposure). The NEMO-3 detector [47] is cylindrical in design. The source foils are in the form of very thin strips (40 to 60 mg/cm^2) and are fixed vertically. It corresponds to a large cylinder of 3.1m in diameter and 2.5m in height (≈ 20 m^2). On both sides of the sources, there is a gaseous tracking detector (mostly Helium gas) which consists of 6180 open drift cells operating in the Geiger mode allowing three-dimensional track reconstruction. A delay electronic allows to record a delay alpha particle in order to detect the electron delay alpha cascade from the ^{214}Bi contamination inside the tracking detector. The wire chamber is surrounded by a calorimeter which consists of 1940 plastic scintillator blocks coupled to very low radioactive photomultipliers (PMT's). For 1 MeV electrons, the energy resolution is FWHM $= [14-17]\%/\sqrt{\mathrm{E(MeV)}}$ and the timing resolution is $\sigma = 250$ ps. The detector response to the summed energy of the two electrons from the $\beta\beta0\nu$ signal is a peak broadened by the energy resolution of the calorimeter and fluctuations in electron energy losses in the source foils, which gives a non-Gaussian tail extending to low energies. The FWHM of the expected $\beta\beta0\nu$ two-electron energy spectrum for ^{100}Mo is about 350 keV. A solenoid surrounding the detector produces a 25 Gauss magnetic field in order to distinguish electrons from positrons. External iron shield, water shield and wood shield cover the detector to reduce external γ and neutrons. Radon-free air, produced by a radon trapping facility, is flushed inside the shield in order to reduce external Radon, and therefore reduce the radon activity inside the tracking chamber.

The sources of backgrounds relevant to the $\beta\beta0\nu$ search in ^{100}Mo and ^{82}Se in NEMO-3 are the irreducible background from its $2\nu\beta\beta$ decay, as well as the decays of ^{214}Bi and ^{208}Tl originating from the natural decay chains of ^{238}U and ^{232}Th. The background isotopes can either be present in the $\beta\beta$ source foils, or can result from ^{222}Rn or ^{220}Rn emanation inside the tracking chamber. ^{214}Bi and ^{208}Tl are progenies of ^{222}Rn and ^{220}Rn respectively and can end up on the surfaces of the source foils and drift cell wires located in the vicinity of the foils. The Thoron contamination is generally much lower than Radon due to its short half-life which

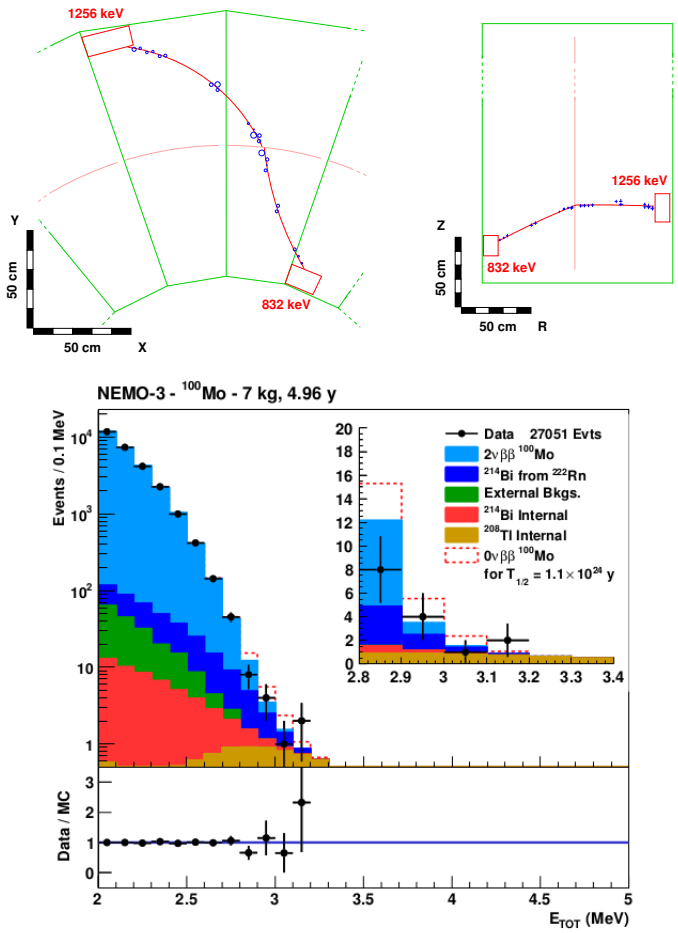

Figure 11. (Top) Transverse and longitudinal display of a reconstructed $\beta\beta0\nu$ candidate event selected from the NEMO-3 data: electron tracks and associated scintillators are well identified; (Bottom) Result of the NEMO-3 experiment with 34.7 kg.y exposure of ^{100}Mo (from [49]).

limits its diffusion capacity. An important feature of NEMO-3 detector is that the different components of background are measured directly using dedicated topology of events since the NEMO-3 detector can identify electrons, positrons, gamma rays and delayed alphas with the combination of the tracking detector, the calorimeter and the magnetic field. A full description of the background analysis is given in reference [48]. The total ^{222}Rn activity inside the tracker chamber was measured to be about 5 mBq/m^3 after the installation of the Radon Trap facility. The ^{220}Rn activity was found to be at a negligible. The Mo source foil contamination activities were measured to be about 100 μBq/kg in ^{208}Tl and between 60 to 300 μBq/kg in ^{214}Bi, depending of the type of Mo foils.

Figure 11 shows the tail of the energy sum distribution of two electrons events emitted from ^{100}Mo source, in the $\beta\beta0\nu$ energy region, after 34.7 kg.yr of ^{100}Mo exposure. In the energy window of $[2.8 - 3.2]$ MeV (around the $Q_{\beta\beta}$-value), the expected number of background events is 18.0 ± 0.6 events (5.2 events from radon contamination; 1.0 and 3.3 events from internal Bi and Tl contamination inside the foil respectively, and 8.45 events from $\beta\beta2\nu$ decay) and 15 events are observed. The $\beta\beta0\nu$ detection efficiency is 4.7%. The limit on the $\beta\beta0\nu$ half-life is $T^{0\nu}_{1/2} > 1.1\ 10^{24}$ yrs (90%C.L.) [49].

9.2. The SuperNEMO experiment

The new SuperNEMO experiment is based on an extension and an improvement of the experimental technique used in the NEMO-3 detector, by combining calorimetry and tracking. The goal is to accommodate about 100 kg of enriched $\beta\beta$ isotope in order to reach a sensitivity of 10^{26} years on the $\beta\beta0\nu$ half-life [50]. The SuperNEMO design is a planar geometry (see Figure 12). The current design envisages about twenty identical modules, each housing 5 kg of enriched $\beta\beta$ isotope. The source is a thin (40 mg/cm^2) foil inside the detector. It is surrounded by a gas tracking chamber followed by calorimeter walls. The tracking volume contains 2000 wire drift cells operated in Geiger mode which are arranged in nine layers parallel to the foil. The calorimeter is divided into around 450 large plastic scintillator blocks which cover most of the detector outer area and are coupled directly to 8" low radioactive PMT's. An energy resolution (FWHM) of 8% at 1 MeV has been measured with prototype, which is a factor two of improvement compared to NEMO-3. The baseline for SuperNEMO is to measure is ^{82}Se: it is relatively easy to enrich by centrifugation (5 kg have been already enriched for the first module), its $Q_{\beta\beta} = 3$ MeV is large and its $\beta beta2\nu$ half-life is 14 times higher than ^{100}Mo. Therefore, taking into account the improvement of the energy resolution, the $\beta beta2\nu$ background will be almost 30 lower than in NEMO-3. Two other isotopes are also investigated: ^{150}Nd and ^{48}Ca. Both isotopes are very promising because they have a large $Q_{\beta\beta}$ value above the ^{214}Bi (Radon) background for ^{150}Nd and above the ^{214}Bi and ^{208}Tl background for ^{48}Ca. They also have a reduced $\beta beta2\nu$ decay (due to Coulomb screening in the case of ^{150}Nd). However their enrichment in large amount is today not available. A R&D program is in progress in Russia in order to enrich large amounts of ^{150}Nd by centrifugation at ultra high temperature and first kilograms could be enriched in the next year. Another R&D program is also in progress in South Korea to enrich ^{48}Ca (1 kg within 3 years) by laser isotope separation.

In order to reach the expected sensitivity of SuperNEMO with ^{82}Se, the Radon contamination inside the tracking detector and the ^{208}Tl contamination in the source foil and measured in NEMO-3, must be reduced by a factor ≈ 50 in SuperNEMO. The radiopurity of the source foils must be $A(^{208}\text{Tl}) < 2$ μBq/kg and $^{214}\text{Bi} < 10\mu$Bq/kg. Such level of radiopurity cannot be measured by standard HPGe gamma spectroscopy. Therefore the SuperNEMO collaboration has developed a dedicated planar detector, named BiPo detector, (3.6 m^2 of active surface) in order to measure and validate the radiopurity of the First SuperNEMO source foils. This BiPo detector is now running in Canfranc Underground Laboratory and measures the first SuperNEMO foil samples at the required radiopurity level. The Radon activity in the tracking detector must be below 0.1 mBq/m^3. Special attentions have been made in the design of the detector tightness and on the selection of the materials inside the tracking detector in order to avoid emanation. The first SuperNEMO module is in construction. It will be installed in LSM in 2015 for first data taking expected end of 2015. If the required level of background is reached, then 20 modules could be installed in the new LSM lab foreseen in the next years.

10. Conclusions

We are today in a period of intense activities with a large variety of $\beta\beta$ experiments, starting to take data or in the construction phase. These projects aim to demonstrate the capability to reduce the background by at least one order of magnitude with at least 100 kg of isotope. We emphasize that the search of $\beta\beta0\nu$-decay requires several experimental techniques and more than one isotope. This is because there could be unknown background and gamma transitions, and a line observed at the end point in one isotope does not necessarily imply that $\beta\beta0\nu$ decay was discovered. Nuclear matrix elements are also not very well known. We must also always keep in mind that every time one starts running a new $\beta\beta$ detector, a new background (unexpected or not) is found. If the required level of background is reached, the new $\beta\beta$ experiments will be able to explore partly or totally the region of expected $\beta\beta0\nu$ signal in the case of inverted

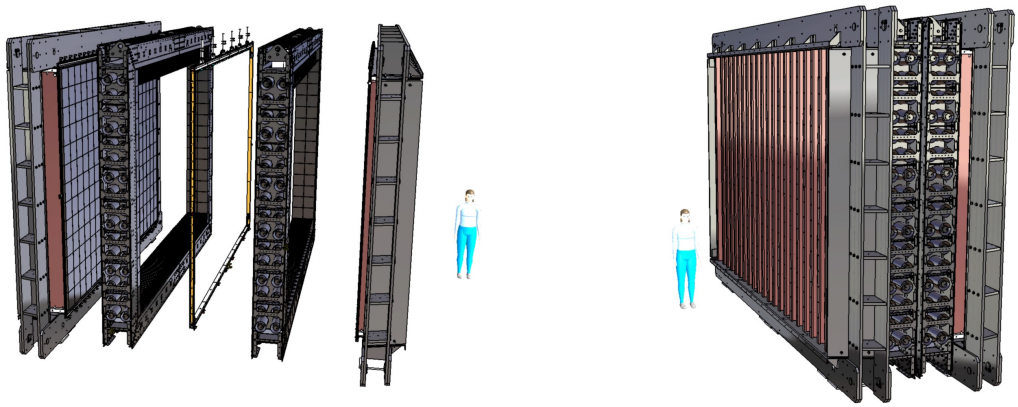

Figure 12. Schematic view of a SuperNEMO module (for a total of 20 modules): Exploded view (left) with the central frame containing the $\beta\beta$ source foil, the two tracking frames and the two calorimeter walls; view (right) of the closed module.

neutrino mass hierarchy (10 meV $< \langle m_{ee} \rangle <$ 50 meV). We remind that other mechanisms, like right handed electroweak current, could also contribute and thus could increase the $\beta\beta0\nu$-decay rate.

References

[1] Nakamura K *et al.* 2010 *Particle Data Group (http://pdg.lbl.gov), JP* G **37** 075021
[2] E. Majorana 1937 *Nuovo Cim.* **14** 171
[3] C. Giunti and C.W. Kim 2007 *Fondamentals of neutrino physics and astrophysics*, Oxford Univ. Press
[4] B. Kayser, *The physics of massive neutrino*, *World Scientific Lecture Notes in Physics* **25**
[5] R.N. Mohapatra and G. Senjanovic 1980 *Phys. Rev. Lett.* **44** 912; R.N. Mohapatra and G. Senjanovic 1981 *Phys. Rev.* D **23** 165; W. Rodejohann, PRAMANA 2009 *(Journal of Phys., Indian Academy of Sciences)* **72** No. 1 217
[6] W. Rodejohann 2011 *Int. Journal of Modern Physics* E **20** 1833
[7] J. Schechter and J.W.F. Valle 1982 *Phys. Rev.* D **25** 2951
[8] S.M. Bilenki and C. Giunti, *arXiv:1203.5250*
[9] A. Dueck, W. Rodejohann and K. Zuber 2011 *Phys. Rev.* D **83** 113010
[10] S. Umehara *et al.* 2008 *Phys. Rev.* C 78, 058501
[11] M. Agostini *et al.* 2013 *Phys. Rev. Lett.* **111** 122503
[12] L. Simard, NEMO-3 Collaboration, presentation given at the 12th Int. Conf. on Topics in Astroparticle and Underground Physics (TAUP 2011), Sept. 2011, Munchen, Germany
[13] R. Arnold *et al.* 2010 *Nucl. Phys.* A **847**, 168
[14] F.A. Danevich *et al.* 2003 *Phys. Rev.* C **68** 035501
[15] E. Andreotti *et al.* 2011 *Astropart. Phys.* **34** 822
[16] A. Gando *et al.* 2013 *Phys. Rev. Lett.* **110** 062502
[17] M. Auger *et al.* 2012 *Phys. Rev. Lett.* **109** 032505
[18] J. Argyriades *et al.* 2009 *Phys. Rev.* C **80** 032501
[19] E. Fiorini *et al.* 1967 *Phys. Lett.* B **25** 602
[20] H.V. Klapdor-Kleingrothaus *et al.* 2001 *Eur. Phys. J.* A **12** 147
[21] C. E. Aalseth *et al.* 2002 *Phys. Rev.* D **65** 092007
[22] K.H. Ackermann *et al.* 2013 *Eur. Phys. J.* C **73** 2330
[23] M. Agostini *et al.* 2013 *J. Phys. G: Nucl. Part. Phys.* **40** 035110
[24] B. Majorovits, *Int. Workshop on Double Beta Decay and Neutrinos, Osaka, Japan, 14-17 November 2011.*
[25] S. Elliot *et al.* 2010 *Phys. Rev.* C **82** 054610
[26] E. Fiorini and T. Niinikoski 1984 *NIM* **224** 83
[27] C. Arnaboldi *et al.* 2003 *Phys. Lett.* B **557** 167
[28] C. Arnaboldi *et al.* 2004 *Nucl. Instrum. Meth.* A **518** 775
[29] M. Vignati on behalf of CUORE Collaboration, talk presented at TAUP-2013 Conference (2013)

[30] J.W. Beeman *et al.* 2012 *Phys. Lett.* B **710** 318
[31] J.W. Beeman *et al.* 2012 *Eur. Phys.J.* C **72** 2142
[32] C. Arnaboldi *et al.* 2011 *Astroparticle Physics* **34** 797
[33] J.W. Beeman *et al.* 2012 *Astropart. Phys.*
[34] C. Arnaboldi *et al.* 2011 *Astroparticle Physics* **34** 344
[35] R.S. Raghavan 1994 *Phys. Rev. Lett* **72** 1411
[36] S. Abe *et al.* 2010 *Phys. Rev.* C **81** 025807
[37] A. Gando *et al.* 2012 *Phys. Rev.* C **85** 045504
[38] M.C. Chen, *Nucl. Phys. Proc. Suppl.* 2005 **145** 65
J Hartnell for *the SNO+ collaboration, arXiv:1201.6169*
[39] L. Winslow, *arXiv:1307.2929*; C. Aberle *et al.*, *arXiv:1307.5813*
[40] E. Conti *et al.* 2003 *Phys. Rev.* B **68**, 054201
[41] J.J. Gomez-Cadenas *et al.* 2012 *JINST* **7** C11007
J.J. Gomez-Cadenas *et al.*, *arXiv:1307.3914*
[42] V. Alvarez *et al* 2013 *JINST* **8** P04002
[43] V. Alvarez *et al.* 2013 *JINST* **8** T01002
[44] E. der Mateosian, M. Goldhaber 1966 *Phys. Rev.* **146** 810
R.K. Bardin *et al.* 1967 *Phys. Lett.* B **26** 112
[45] I. Ogawa *et al.* 2012 *Journal of Physics: Conference Series* **375** 042018
http://iopscience.iop.org/1742-6596/375/4/042018
[46] T. Bloxham *et al.* 2007 *Phys. Rev.* C **76** 025501
K. Zuber 2001 *Phys. Lett.* B **519** 1
[47] R. Arnold *et al.* 2005 *Nucl. Instr. and Meth.* A **536** 79
[48] R. Arnold *et al.* 2009 *Nucl. Instr. and Meth.* A **606** 449
[49] R. Arnold *et al. arXiv:1311.5695*
[50] R. Arnold *et al.* 2010 *Eur. Phys. J.* **70** 927